

Article

Field Study on Impact of Mechanical Pressurization on Pressure Distribution in High-Rise Buildings

Kyung-Hwan Ji ¹, Su-Ji Choi ²  and Jae-Hun Jo ^{3,*}

¹ Industrial Science and Technology Research Institute, Inha University, Incheon 22212, Republic of Korea; kkinghwan@naver.com

² Department of Architectural Engineering, Inha University, Incheon 22212, Republic of Korea; suji2990@gmail.com

³ Division of Architecture, Inha University, Incheon 22212, Republic of Korea

* Correspondence: jhjo@inha.ac.kr; Tel.: +82-32-860-7582

Abstract: In high-rise buildings, the excessive pressure differences cause various problems, and architectural and mechanical measures are always applied. In this study, pressure measurements on a 67-story high-rise building were conducted to evaluate the effect of mechanical pressurization on the pressure distribution. Absolute pressure measurement devices were installed at 28 points on 10 floors, a full-scale pressure profile of the test building was derived, and the pressure distributions on the main floors were reviewed. Four pressurization modes for the test building were considered, and the variation in the pressure distribution for each mode was analyzed. The results showed that mechanical pressurization reduced the pressure difference on the lobby floor by approximately 18%. Although it did not exert an apparent impact on the pressure difference due to the stack effect, pressurizing the entire floor serves as the most effective way of reducing the excessive pressure difference.

Keywords: stack effect; mechanical pressurization; high-rise building; pressure difference; pressure distribution



Citation: Ji, K.-H.; Choi, S.-J.; Jo, J.-H. Field Study on Impact of Mechanical Pressurization on Pressure Distribution in High-Rise Buildings. *Buildings* **2023**, *13*, 3039. <https://doi.org/10.3390/buildings13123039>

Academic Editor: Apple L.S. Chan

Received: 14 November 2023

Revised: 30 November 2023

Accepted: 2 December 2023

Published: 6 December 2023



Copyright: © 2023 by the authors. Licensee MDPI, Basel, Switzerland. This article is an open access article distributed under the terms and conditions of the Creative Commons Attribution (CC BY) license (<https://creativecommons.org/licenses/by/4.0/>).

1. Introduction

In recent years, with the increase in the number of high-rise buildings in Korea, various problems related to pressure distribution have occurred. In general, an excessive pressure difference is produced in high-rise buildings, particularly on the envelopes and internal partitions of the buildings, due to the comprehensive influence, including the stack effect, external wind pressure, and mechanical pressure [1]. The pressure difference causes various problems, such as malfunction of the elevator doors, noise problems, energy loss due to infiltration, the diffusion of indoor pollutants and bacteria, and thermal discomfort. The excessive pressure difference in the elevator door generates unpleasant noise through door cracks and may result in malfunction of the elevator door, particularly on the top and bottom floors of elevator shafts [2–8]. In addition, the excessive pressure difference can also accelerate the spread of smoke and fire through vertical paths, such as elevator shafts and stairwells [9].

Several methods have been proposed in existing studies to address and mitigate excessive pressure differences in high-rise buildings. Jo et al. [10] and Loveatt et al. [11] suggested that architectural improvements should be considered in the building design stage, such as improving the airtightness levels of the building envelope and designing indoor partitions to reduce the pressure difference by controlling the infiltration. However, these architectural measures are only feasible for new buildings, which is a challenge for existing structures due to construction complexities and high economic costs. Therefore, in recent high-rise buildings under construction, architectural improvement is being considered at the design stage. However, it needs to be noted that a significant pressure difference

still persists between the elevator shafts of the top and bottom floors of high-rise buildings, despite the application of these mentioned measures.

In addition, research on facility improvements applied to high-rise buildings has also been conducted, primarily driven by challenges associated with applying architectural improvements to the existing buildings. The main principle of these methods is to reduce the magnitude of the pressure difference by lowering the temperature difference between the shaft and the external environment. This can be achieved through techniques such as drawing outdoor air into the elevator shaft using a fan [12] or implementing a passive cooling system for the elevator shaft [13–15]. For example, Yu et al. [16] performed a set of simulation cases to find an effective HVAC operation scheme to reduce the excessive pressure difference acting on building components, and the scheme of pressurizing the upper zone of a building was implemented in the actual building. In addition, they also put forward various operation modes for the HVAC systems to solve the unpleasant noises due to the stack effect. Even though the mode of pressurizing the high-rise zone of the building based on the outdoor air temperature and wind velocity effectively reduced the noise level, the indoor environment of the high-rise zone changed significantly [17]. However, there are limitations to these methods, such as the energy loss and potential discomfort caused by cold drafts entering from the shafts into indoor spaces [18]. It is important to note that these operation modes of the pressurization systems can only be applied to the target buildings studied, and the actual effectiveness of all kinds of HVAC operation modes needs to be evaluated comprehensively.

Considering the difficulty in mitigating the stack effect with a single improvement method, combinations of architectural and mechanical measures have also been proposed by some researchers [14,19]. However, it should be noted that there are always antagonistic or negative effects among different improvement methods [19]. Li et al. [14] evaluated the practical applicability of the countermeasures applied in the high-rise office building for the final decision-making and put forward a reasonable ranking for various combinations of the improvement methods. In addition, due to the limitations of on-site construction and the lack of practical application, the application of the combination of improvement methods in actual high-rise buildings is still difficult.

In this study, the effect of pressurization by mechanical systems on the pressure distribution in a high-rise building was evaluated based on field measurements. To determine the pressure distribution throughout the test building, self-developed absolute pressure measuring devices were installed at 28 points on 10 floors of a 67-story high-rise office building. The full-scale pressure distribution profile of the building and the pressure distribution on the main floors were obtained. In addition, the impact of the mechanical pressurization was assessed by considering four pressurization modes applied to the test building, and the pressure difference for each mode and the pressure distribution profile of the entire building were then evaluated.

2. Pressure Difference in Buildings

2.1. Driving Forces

Pressure distribution in high-rise buildings is essential for the normal operation of various functions based on airflow patterns, such as the operation of HVAC systems, smoke control, and elevator systems. The airflow patterns within buildings are affected by a combination of pressure differences induced by the stack effect (ΔP_{st}), wind (ΔP_w), and mechanical systems (ΔP_{mech}). The total pressure difference (ΔP_{total}) caused by the combined forces can be expressed using Equation (1) [1].

$$\Delta P_{total} = \Delta P_{st} + \Delta P_w + \Delta P_{mech} \quad (1)$$

2.1.1. Stack Effect Pressure (ΔP_{st})

The stack pressure is the main driving force of air movements within high-rise buildings, resulting from the variation in air density primarily due to temperature differences

within the interiors of the building. Assuming that the air temperature and humidity ratio are constant over the building height, the stack pressure decreases linearly with an increase in the distance from the reference point. In high-rise buildings, significant density differences arise from temperature variations between indoor and outdoor environments, which causes the stack pressure difference that drives the outdoor airflow into the building through openings on the lower floors. Therefore, the stack pressure difference is a function of the building height and temperature difference, and the magnitude of the stack effect increases with increasing height and temperature difference, as shown in Equation (2) [20].

$$\Delta P_{st} = (\rho_o - \rho_i)g(H_{NPL} - H) = \rho_o\left(\frac{T_i - T_o}{T_i}\right)g(H_{NPL} - H), \quad (2)$$

where ΔP_{st} is the stack pressure difference (Pa), ρ_o is the outdoor air density (kg/m^3), ρ_i is the indoor air density (kg/m^3), g is the gravitational acceleration (m/s^2), H_{NPL} is the height of the neutral pressure level (NPL) above the reference plane without any other driving forces (m), T_i is the absolute indoor temperature (K), and T_o is the absolute outdoor temperature (K). In particular, the H_{NPL} is the vertical location in the building where the indoor and outdoor air pressures are balanced for all the buildings, which is influenced by interior components, such as walls and floor partitions, and vertical shafts, such as elevators and stairwells. Previous research [21] has shown that the NPL is typically located between 0.3 and 0.7 times the total building height.

2.1.2. Wind Pressure (ΔP_w)

The wind pressure is another driving force causing pressure differences in buildings, as shown in Equation (3) [20]. The positive pressure difference typically occurs on the windward side of a building, allowing air to flow into the building through openings and gaps. The negative pressure difference occurs in opposite directions and on the roof, leading to air flowing out of the building. Due to the non-continuous and inconsistent characteristics of the wind effect, the effects of wind are intermittent and highly variable [22].

$$\Delta P_w = C_p \rho \frac{U^2}{2}, \quad (3)$$

where P_w is the wind pressure relative to the outdoor static pressure in undisturbed flow (Pa), C_p is the wind pressure coefficient (dimensionless), ρ is the outdoor air density (kg/m^3), and U is the wind speed (m/s). The pressure coefficient, C_p , depends on the building shape, the wind direction, and the influence of nearby buildings, vegetation, and terrain features. The C_p is generally positive on windward surfaces and negative on leeward surfaces. Furthermore, the wind speed, U , is estimated by applying terrain and height corrections to the hourly wind speed from a nearby meteorological station.

2.1.3. Mechanical Pressure (ΔP_{mech})

Mechanical systems control the temperature and humidity of a target space primarily through fan-driven airflows to adjust the building environment. The mechanical systems in buildings are generally classified into two main categories: constant-flow systems (CAV) and variable-flow systems (VAV), which adjust the indoor environment by supplying, exhausting, and returning air.

A mechanical system can be regulated by utilizing fans to control the pressure difference between the supply and the return air, as measured by sensing mechanisms (Figure 1). Consequently, it can either depressurize the target space by increasing the supply air volume or reducing the return air volume, or it can pressurize it by decreasing the supply air volume or increasing the return air volume. The pressurization/depressurization methods allow the room pressure to be adjusted using positive or negative pressure difference rather

than zero pressure. The equation for calculating the airflow using pressure difference sensing is expressed as Equation (4).

$$Q_r = Q_{sup} - (Q_{ext} + Q_{inf}), \tag{4}$$

where Q_r is the return airflow (m^3/h), Q_{sup} is the supply airflow (m^3/h), Q_{ext} is the exhaust airflow (m^3/h), and Q_{inf} is the infiltration airflow (m^3/h).

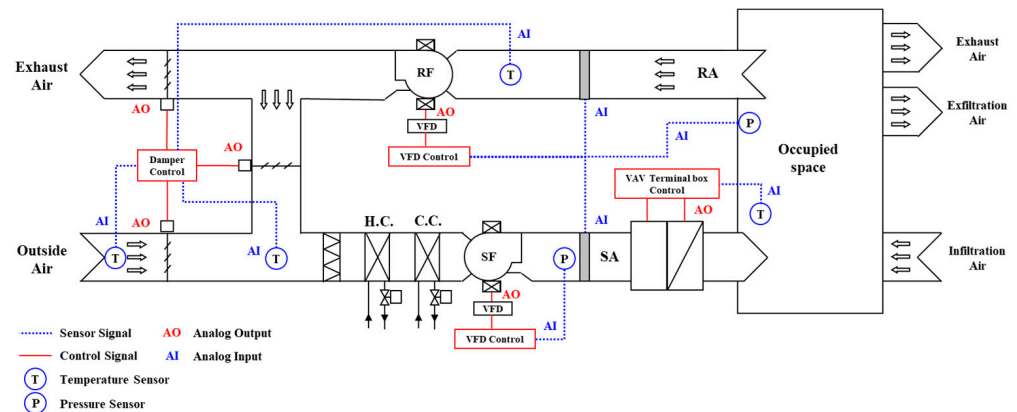


Figure 1. Building pressure control through pressure difference sensing.

2.2. Full-Scale Pressure Profile in High-Rise Buildings

As shown in Section 2.1, the driving forces, including the stack effect, wind, and mechanical pressures, generate pressure differences between zones in buildings, resulting in airflow. In high-rise buildings, particularly during winter and when the outside temperature is low, the stack effect becomes dominant, leading to the significant pressure difference that drives the primary airflows. In general, the airflows always flow into the buildings on the lower floors of the high-rise buildings and flow out of the buildings above the NPL. Previous studies [23,24] have predicted the pressure profiles of an entire building with a single elevator shaft, as shown in Figure 2a, and the pressure distribution profile of a high-rise building with multi-zone elevator shafts was derived by field measurements, as shown in Figure 2b.

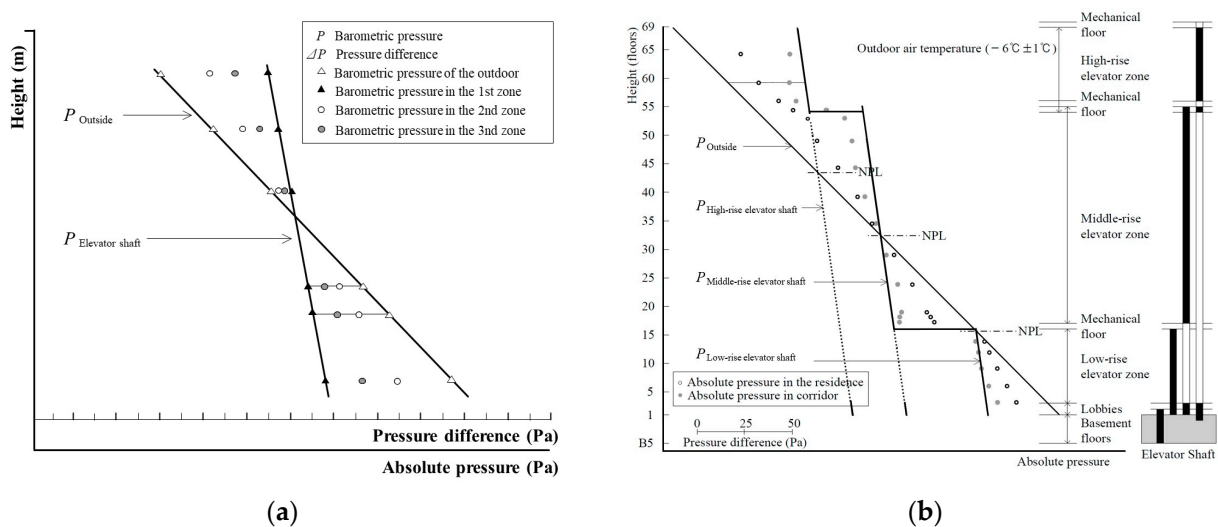


Figure 2. Pressure profile in high-rise buildings. (a) Pressure profile due to the stack effect. (b) Pressure profile in multi-zone shaft building.

Jo et al. [24] predicted the vertical pressure distribution by considering variables such as the indoor–outdoor temperature difference, the elevator shaft height, the shaft NPL height, and the horizontal pressure distribution by considering the airtightness of the external and internal walls on the plan. The proposed method assumed similar floor plans and indoor temperatures for all floors, but actual buildings have more complex floor plans and indoor environmental conditions. Therefore, they proposed a method for deriving the pressure distribution profile based on the pressure data collected from the main reference zone (Figure 3a), which involves two steps.

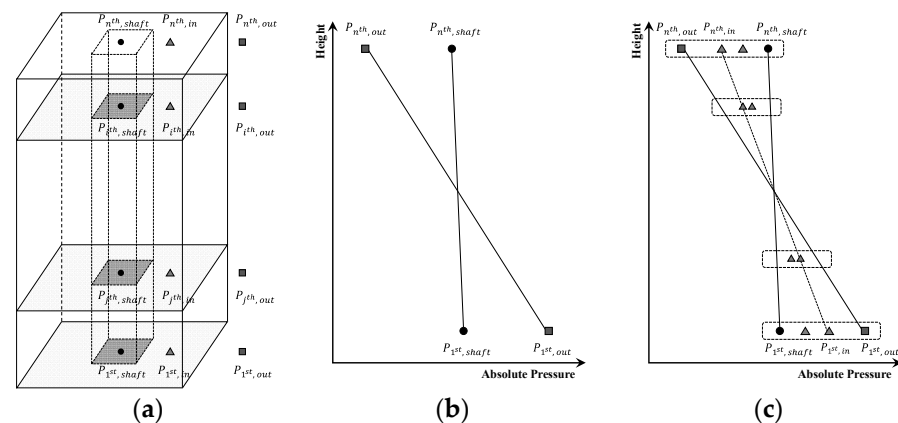


Figure 3. Procedure for deriving pressure profiles. (a) Measurement of absolute pressure. (b) Step 1. (c) Step 2.

Step 1: Measurement of vertical pressure distribution

The maximum pressure difference in the building was measured to derive the vertical stack pressure profile, which was determined by measuring the pressure difference between the building outside and the passenger elevator shaft. The vertical pressure distribution was obtained by measuring the outside pressure on the lowest and highest floors and the pressure in the passenger elevator shaft, as shown in Figure 3b. When the elevator shaft is divided into multiple zones, the vertical pressure distribution is derived by measuring multiple reference data.

Step 2: Measurement of horizontal pressure distribution

The pressure difference between the zones was determined by measuring the absolute pressure in each zone of the main floor (lobby, lowest, and highest floors of each elevator shaft). The pressure distribution on the other floors was derived by determining the pressure distribution ratio (e.g., TDC) between the zones through multiple measurements (Figure 3c).

3. Field Measurement of Pressure Profile

In order to evaluate the impact of the mechanical system on the pressure distribution, it is necessary to derive the pressure profile in the building. To obtain a full-scale pressure profile, pressure measurements were performed on a high-rise building using a self-made absolute pressure measuring device, according to the method described in Section 2.2. The pressure distribution ratios were calculated based on the measured pressures to determine the pressure distribution throughout the entire building, which was then utilized to derive a full-scale pressure profile.

3.1. Test Building Summary

To investigate the impact of a mechanical system on the pressure difference in a high-rise building, the pressure distribution was measured in a fully completed office building located in Seoul. The test building contains 7 basement floors and 67 floors above ground, and the total height is 317.7 m. The test building was divided into four vertical zones: the

lobby zone (B1–1F), the lower zone (2F–29F), the middle zone (30F–50F), and the upper zone (51F–66F). An overview of the target buildings is presented in Table 1.

Table 1. Summary of the test office building.

Picture	Classification	Description
	Location	Seoul, Republic of Korea
	Completion year	2016
	Building usage	Office
	Number of floors above ground	67
	Number of basement floors	7
	Building height	317.7 m

3.2. Pressure Data Collection in the Test Building

Self-developed absolute pressure monitoring systems were installed to monitor absolute pressure in real time. The real-time absolute pressure monitoring system comprised a data receiver, a logger (system A), and pressure sensors (system B), as shown in Table 2.

Table 2. Specifications of absolute pressure measurement devices.

Device	Picture	Specifications
Data receiver and logger (Pressure monitoring system A)		Communication Function RF communication receive real-time measured data from multiple B systems
Pressure sensors (Pressure monitoring system B)		Model Range Accuracy Repeatability Interval Function Model PTB110 800 to 1100 hPa ± 0.30 hPa at $+20$ °C ± 0.03 hPa 5 s (Minimum) monitor real-time absolute pressure and communicate with system A

The building zoning planning was first reviewed using drawings and site reviews of the test building. The test building consists of three elevator shafts, and there are two transit floors. Pressure measurements were conducted using a monitoring system to determine both the vertical and horizontal pressure distributions and to derive a full-scale pressure profile.

To determine the vertical pressure distribution, the devices shown in Table 2 were installed outside the lobby floor (1F) and top floor (66F) as well as inside the passenger elevator shafts of the lowest and highest floors: the lobby floor (1F), the transit floors (32F, 52F), and the top floor (66F). Additional devices were installed at 13F, 22F, 39F, 46F, and 54F to monitor the pressure distribution at the reference floor of each shaft. Consequently, the horizontal pressure distribution was analyzed along the main horizontal airflow paths, where air flowed from the outside to the elevator shaft inside the building. On the lobby floor, the absolute pressure of the outside, Lobby2, Lobby1, and each elevator shaft was measured. On the transit and reference floors, the absolute pressure of the outside, office, each elevator hall, and each elevator shaft were measured to derive the horizontal pressure distribution. The locations of the measuring devices installed to derive the pressure distribution in the test building are indicated in Figure 4.

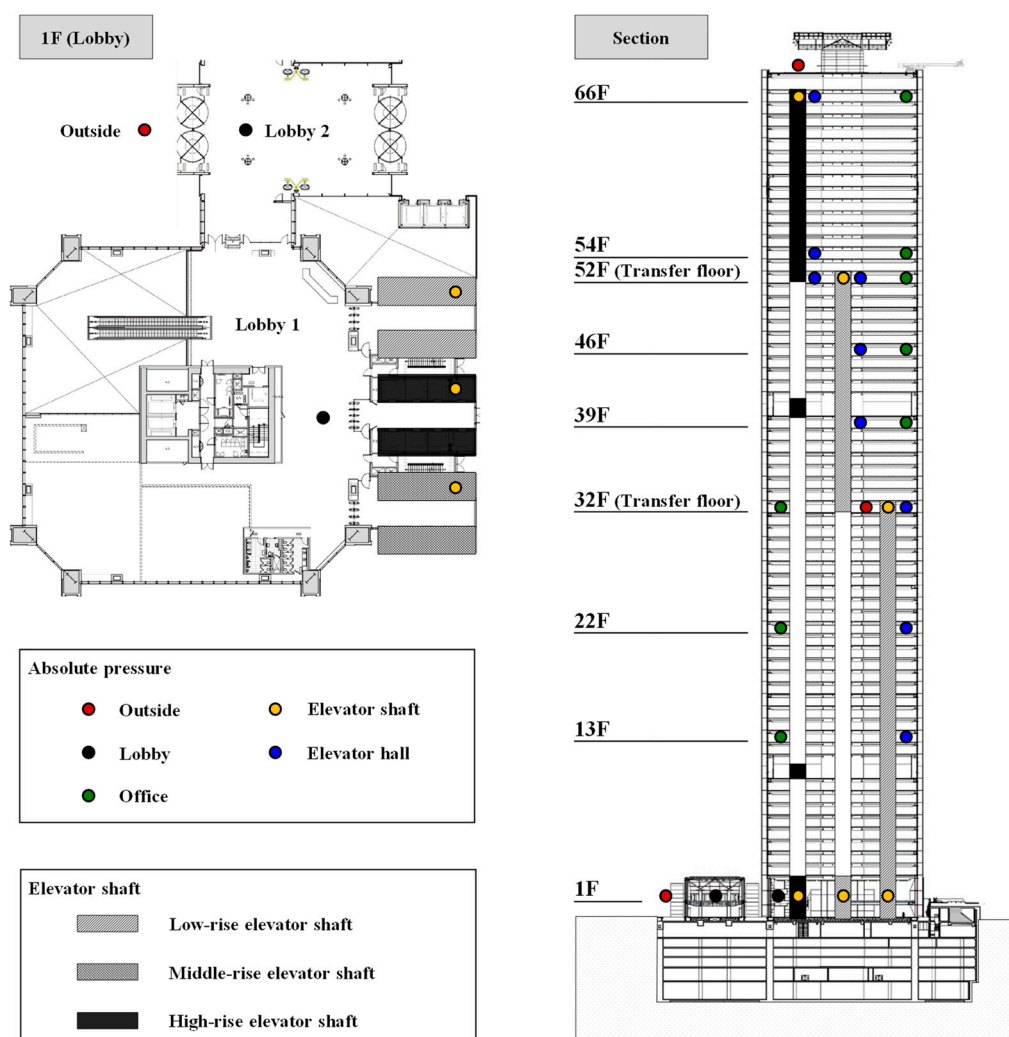


Figure 4. Locations of absolute pressure monitoring systems.

3.3. Measurement Result of Building Pressure

The pressure measurements were conducted during the heating season. During the measurement, the outdoor temperature was around $-14.0\text{ }^{\circ}\text{C}$, and the indoor temperature ranged from 19.0 to $23.0\text{ }^{\circ}\text{C}$. Therefore, the indoor–outdoor temperature difference was approximately $30\text{ }^{\circ}\text{C}$. Figure 5 shows the pressure distribution on the lowest floor (Lobby, 1F) and the highest floor (66F), where the pressure difference was the greatest.

In the elevator shaft, which is the main path for vertical airflows, the largest pressure difference was measured between the lobby floor (1F) and the top floor (66F), where the shaft attains its maximum length. The total pressure difference on the lobby floor was 136 Pa , and that on the top floor was 145 Pa . An analysis of the pressure differences across the main compartments of the lobby floor showed that the pressure difference between Lobby 1 and Lobby 2 was the highest at approximately 78 Pa .

The pressure difference between the outside and Lobby 2 was approximately 1 Pa . This implies that the wall that divided Lobby 2 did not serve as an envelope, while the partition wall of Lobby 1 served as the primary envelope. The pressure difference at each elevator door was measured at 57 Pa . This exceeded the threshold pressure of 40 Pa for elevator malfunctions, as established in a previous study [25], thereby confirming the potential for an issue with the elevator door.

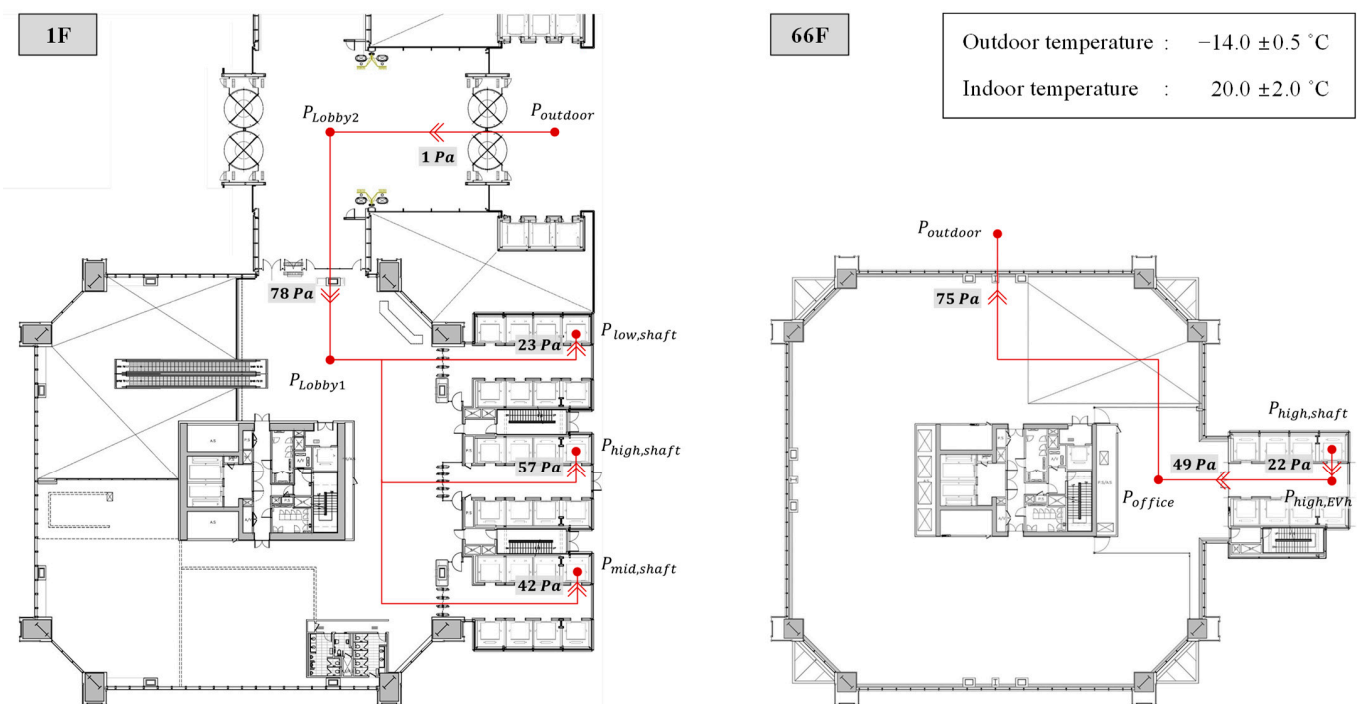


Figure 5. Pressure distribution in the lobby floor and the 66th floor in the base mode.

The TDC value of the lobby floor envelope was measured at approximately 0.57. The lobby floor had a main entrance to the outside but shared a high-pressure difference with the envelope. Based on the assessment of the TDC values, both the envelope and lobby floor doors were tightly constructed. The pressure distribution on the 66th and top floors was measured. The TDC of the curtain wall was as high as 0.51, and the TDC of the hall in front of the elevator was as high as 0.34. It is assumed that both the curtain wall and the elevator hall doors were tightly installed and shared the high-pressure differences across that compartment. Therefore, a low-pressure difference of approximately 22 Pa was measured across the high-rise elevator doors. This low pressure was shared with the elevator doors, thereby avoiding problems such as elevator door malfunctions and noise.

The full-scale pressure profile, derived from the entire measurement dataset, is shown in Figure 6. It displays similar characteristics as those commonly observed in high-rise buildings. The pressure distribution ratios on the reference floor are similar to those on the 66th floor, except for the lobby floor. The TDC values for both the exterior envelope and the elevator lobby partitions were high, resulting in pressure differences on both sides of the elevator doors as low as 30 Pa. The pressure difference was not anticipated to cause issues on the base floor of the test building due to the appropriate pressure distribution ratio between the envelope and the internal compartment. The NPL of a high-rise elevator shaft was measured on the 31st floor, located lower than the midpoint of the shaft, approximately 45% of the shaft height. A typical pressure distribution profile of a multi-zone shaft plan shows that the pressure lines of each shaft are separated independently, as shown in Figure 2b. However, as shown in Figure 6, the pressure lines of each shaft are almost always indistinct in this building. In addition, the pressure difference in the high-rise elevator shaft was measured to be relatively low compared to the pressure difference at the same building height. This tendency is due to the location of the elevator shaft close to the outside air, as shown in the floor plan in Figure 4. Compared to the indoor temperature of 19.0–23.0 °C, the temperature in the elevator shaft was measured to be approximately 7.0–10.0 °C, resulting in a smaller pressure difference due to the relatively lower temperature difference.

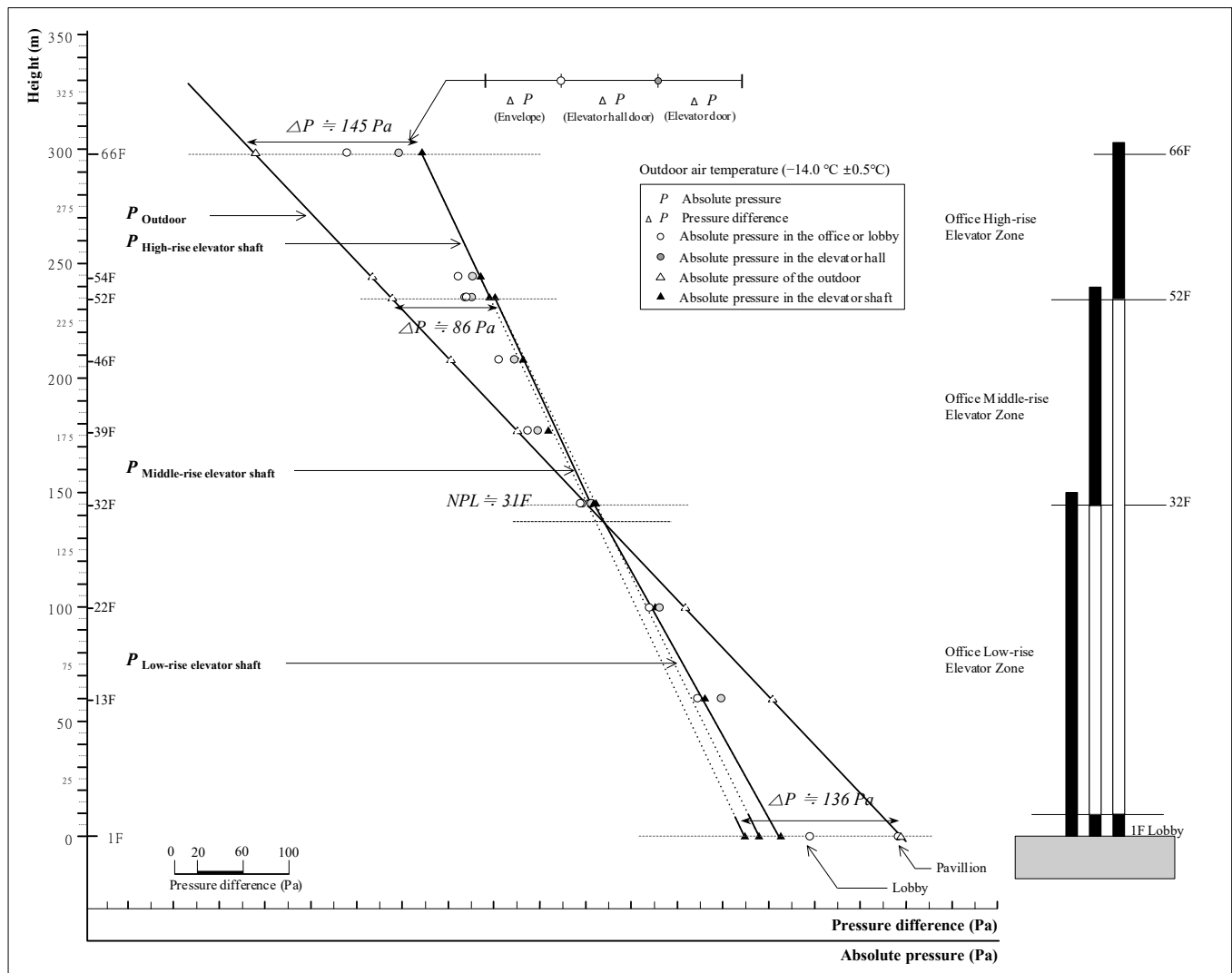


Figure 6. Pressure distribution profile without mechanical pressurization (base mode).

4. Evaluation of Pressurization Impact in the Test Building

4.1. Mechanical System of Test Building

The zoning of the mechanical system in the test building was reviewed to determine its effect on the pressure differences in the mechanical systems. The vertical zoning was divided into the lobby, lower, middle, and upper zones. The mechanical rooms for each zone were located on the 10th, 40th, and 67th floors, respectively. Other air-conditioning facilities, elevator halls, and toilet exhausting facilities were connected vertically. A schematic diagram of the vertical air-conditioning system of the test building is shown in Figure 7.

4.2. Evaluation Pressurization Mode Using Mechanical System

In order to understand the effectiveness and extent of the influence of mechanical pressurization using air-conditioning systems in real buildings, four pressurization modes applied in high-rise buildings were classified. The pressure difference variation when applying the pressurization mode was measured, and the pressurization mode that was most effective at reducing the pressure difference due to the stack effect was reviewed.

This measurement was conducted in an environment similar to the previous profile measurement during the heating season. Table 3 summarizes the schedule for adjusting the air-conditioning system. The pressure difference was measured by modifying the operating conditions of the air-conditioning system in four modes. Each mode was maintained under the same conditions for a duration of 40 min. Due to the large size of the test building, the

effect of pressurization takes a considerable amount of time to appear after a mode change. In the pre-investigation of the pressure control, it was determined that approximately 10 min were needed for pressure stabilization. As a result, a stabilization interval of 20 min was set between each mode in this study. In addition, to maximize the effects of pressurization, when the air-conditioning fans on the corresponding floors were switched off, the exhaust fans of the toilets on that floor were also switched off. The pressure data measured from 02:15 to 02:30 in Mode 3 were excluded from the measurement data for data reliability due to air conditioner control errors.

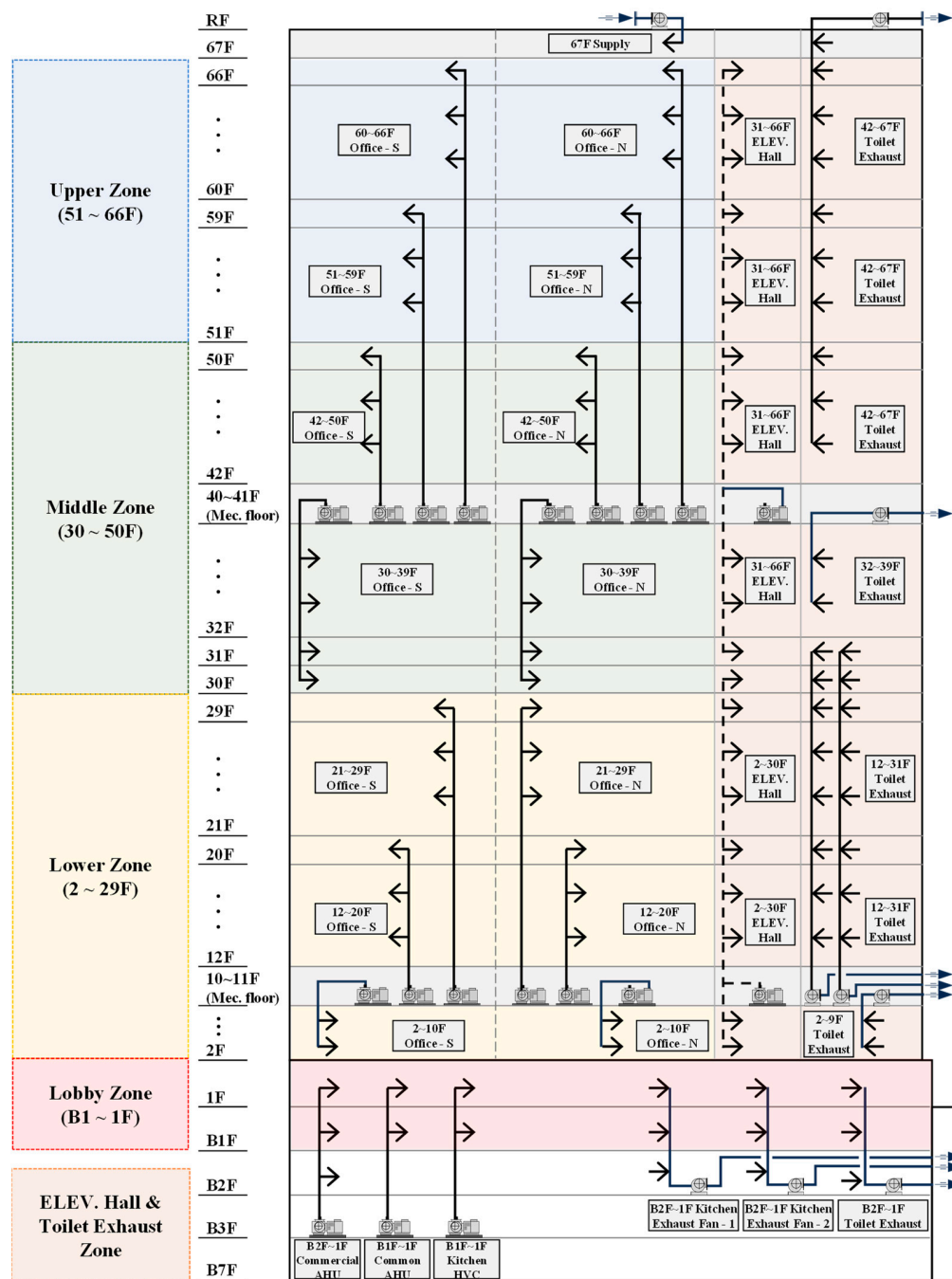


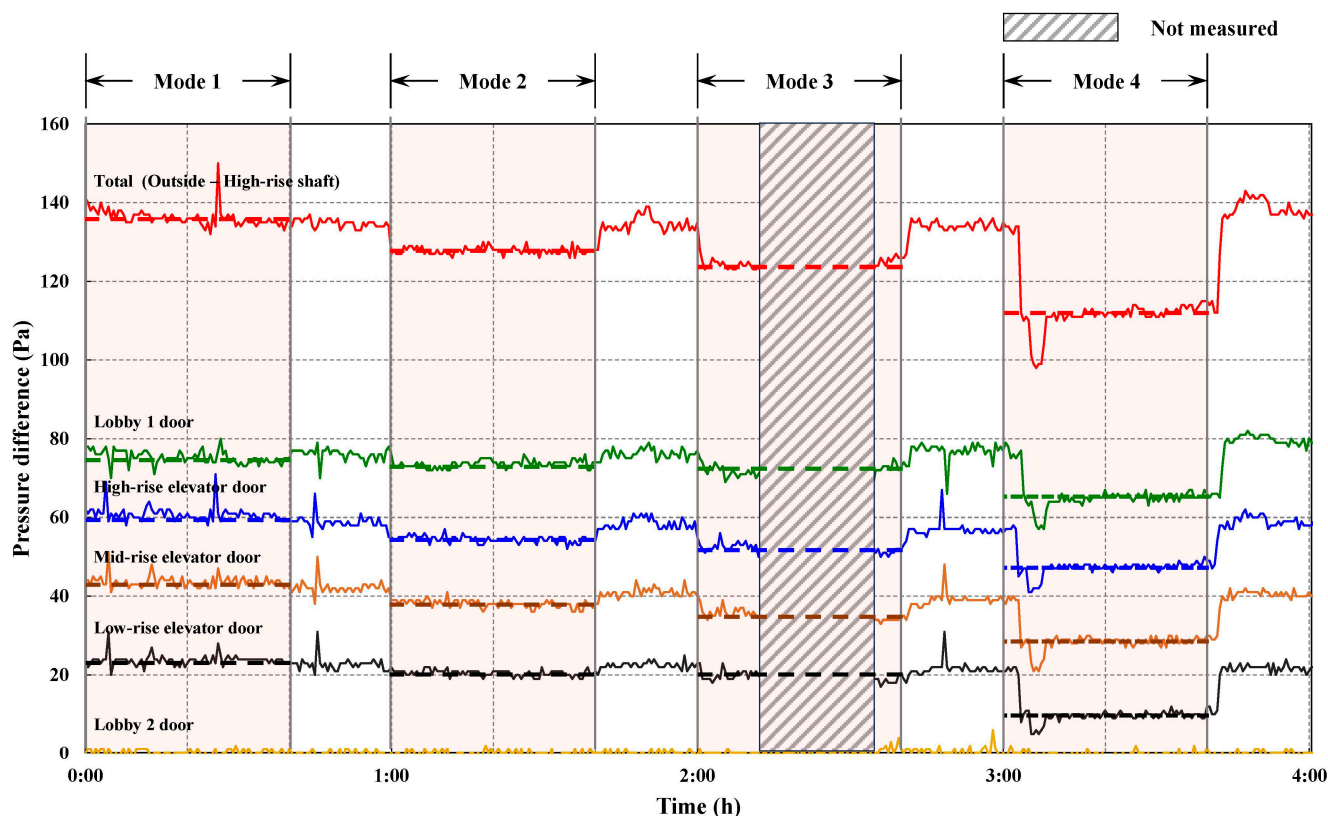
Figure 7. Zoning plan of HVAC system.

Table 3. Pressurization mode using mechanical system.

Classification	Base Mode	Mode 1	Mode 2	Mode 3	Mode 4
Pressurization Zone	-	Lobby zone B1~1F	Upper zone 51~66F	Middle and Upper zone 30~66F	Whole floor zone B1~66F
Floor	-				
Time	-	00:00~00:40	01:00~01:40	02:00~02:40	03:00~03:40
Upper zone area	Supply fan: on Return fan: on	Supply fan: on Return fan: on	Supply fan: on Return fan: off	Supply fan: on Return fan: off	Supply fan: on Return fan: off
Middle zone area	Supply fan: on Return fan: on	Supply fan: on Return fan: on	Supply fan: on Return fan: on	Supply fan: on Return fan: off	Supply fan: on Return fan: off
Lower zone area	Supply fan: on Return fan: on	Supply fan: on Return fan: on	Supply fan: on Return fan: on	Supply fan: on Return fan: on	Supply fan: on Return fan: off
Lobby zone area	Supply fan: on Return fan: on	Supply fan: on Return fan: off	Supply fan: on Return fan: on	Supply fan: on Return fan: on	Supply fan: on Return fan: off

4.3. Impact of Pressurization in Real Building

The mechanical pressurization described in Table 3 was performed at 40-min intervals when the outdoor air temperature was $-14.0\text{ }^{\circ}\text{C}$ (i.e., the temperature point at which the stack effect caused the pressure difference to become significant). The pressures were measured at six points in the lobby area (outdoors, Lobby 2, Lobby 1, lower elevator shaft, mid-level elevator shaft, and upper elevator shaft), and Figure 8 shows the pressure difference as a function of the mode change over time for five areas (lobby 2 door, low-rise elevator door, mid-rise elevator door, high-rise elevator door, and lobby 1 door).

**Figure 8.** Pressure difference in lobby floor (1F).

In order to evaluate the effect of the pressurization mode on the variation in the pressure difference, the pressure difference in the lobby (1F) where most of the pressure difference problems occurred was reviewed. In the base mode, the total pressure difference between the outside and the high-rise elevator shafts was measured to be approximately

136 Pa. In Mode 1, which pressurized the lobby, almost no pressure difference was observed. Meanwhile, in Mode 2, which pressurized the high-rise zone, the pressure difference was 127 Pa, indicating a reduction of approximately 9 Pa. In Mode 3, designed to pressurize the upper and middle floors, the pressure difference was approximately 124 Pa. Furthermore, in Mode 4, which pressurized whole floors, the pressure difference was reduced to 111 Pa, indicating a reduction of approximately 25 Pa and an overall pressure difference reduction of approximately 18%. Therefore, the method of pressurizing whole floors showed the greatest reduction in the pressure difference.

The pressure difference was measured at a high-rise elevator door, where problems caused by an excessive pressure difference are most common, and the pressure difference in the base mode was 58 Pa. The pressure difference was 60 Pa, 54 Pa, 52 Pa, and 46 Pa in Mode 1, Mode 2, Mode 3, and Mode 4, respectively, when mechanical pressurization was applied. Mode 4 was the most effective mode at reducing the pressure difference by about 20% compared to the basic mode, but the pressure difference was more than 40 Pa, which is a problematic pressure difference suggested by a previous study [25].

The TDC variations of the main compartments due to the pressure difference were then evaluated. The TDC value was calculated based on the elevator shaft, which exhibited the highest pressure difference on the lobby floor. Based on the TDC values, the pressure distribution ratio of the Lobby 1 door, identified as the primary envelope, was measured to be approximately 0.55–0.60, while the elevator shaft for the high-rise floors exhibited a value of approximately 0.40–0.45. As shown in Figure 9, the pressure difference in the pressurization mode can be identified; however, the TDC value of each compartment was constant. The TDC values of the data excluded from the analysis were consistent. In general, the pressure distribution ratio of the envelope of the lobby floor was approximately 0.2–0.3 due to the wide podium and many external doors. The test building had a high value of 0.55, indicating that the envelope was more airtight than others. The pressure distribution ratio of Lobby 2 was nearly zero, indicating the very low airtightness of the envelope of Lobby 2. It should be noted that the large change in the TDC value of the lobby 2 door at 00:45 was due to the elevator moving and the door opening during the measurement period, which was not included in the data analysis due to non-compliance with the measurement conditions.

Figure 10 shows the pressure profile when applying full-floor pressurization. Compared to the base mode, the neutral zone of the building decreased from approximately 31 floors (approximately 45% of the building height) to approximately 25 floors (approximately 40% of the building height). In addition, the total pressure difference at the lowest floor decreased and increased at the top floor. However, there was no significant change in the pressure difference between the elevator doors on the reference floors. It was confirmed that the pressure difference can be reduced by applying the pressurization mode when problems related to an excessive pressure difference occur.

The pressure profile for the whole-floor pressurization (Mode 4) was analyzed based on the pressure measurement results of the lobby floor, which showed the best reduction in the pressure difference. As shown in Figure 10, the pressure distribution in the high-rise elevator shaft, where the most problems occurred, shifted to the right. As a result, the height of the NPL decreased from 32 floors (approximately 45% of the building height) in the base mode to about 25 floors (approximately 40% of the building height) in the whole-floor pressurization (Mode 4). In addition, the total pressure difference on the lobby floor (1F) decreased by approximately 24 Pa but increased by approximately 20 Pa on the top floor (66F). The analysis of the pressure distribution ratios of the base floor of the office revealed that the TDC values were high on most of the floors. Due to the high TDC value of the envelope, the pressure distribution ratio of the internal compartments was reduced, and the probability of issues, such as elevator malfunction and noise in the gaps of the internal compartments, was lower on the reference floor.

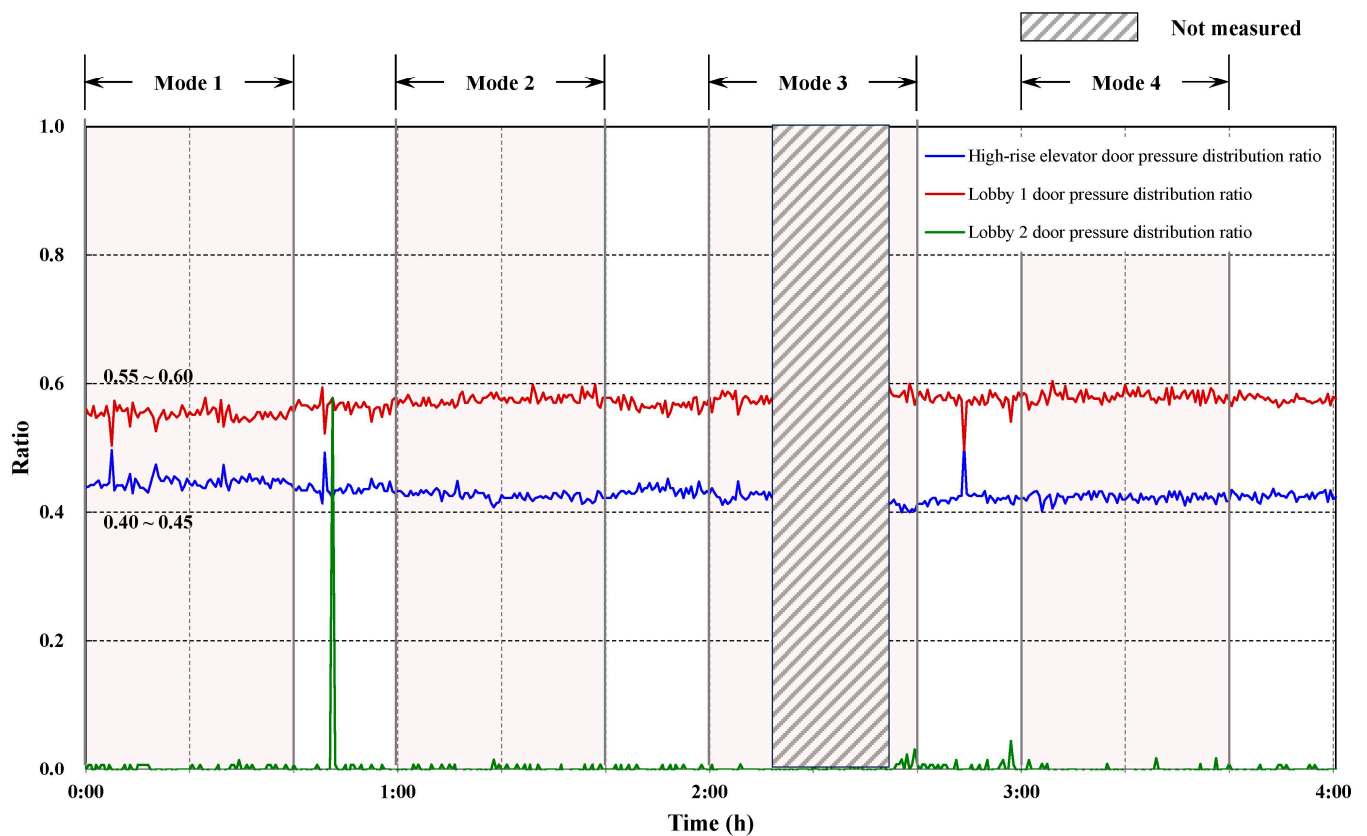


Figure 9. Variation of the TDC value on the lobby floor (1F).

4.4. Discussion and Limitations

The impact of mechanical pressurization on pressure changes in a high-rise building was investigated by measuring the absolute pressure in a 67-story building with the HVAC system not in operation. The pressure difference in the main compartment was calculated using the monitored data to determine the full-scale pressure distribution profile throughout the entire building. The evaluation of the four applicable modes of pressurization in the mechanical system revealed that the method of pressurizing the entire floors was effective at reducing the pressure difference on the lobby floor. However, the reduction in the pressure difference by mechanical pressurization methods is not sufficient to control the stack effect in high-rise buildings due to the dominant influence of stack effect pressures. In relatively low-rise buildings, mechanical pressurization can be effective at controlling chimney effect pressures, and the use of HVAC systems can reduce the pressure difference, as demonstrated in Tamblyn's study [26]. In particular, mechanical pressurization is expected to reduce the pressure difference in cases where the indoor–outdoor temperature difference is small and the height of the buildings is low.

It should be noted that the results of this study are limited to a specific point in time and cannot be generalized to the entire period. In addition, in order to obtain stable measurements, the measurements were conducted at night when the effects of the elevators, occupants, and sunlight were excluded, which suggests that the results differ during the day when the building is in use.

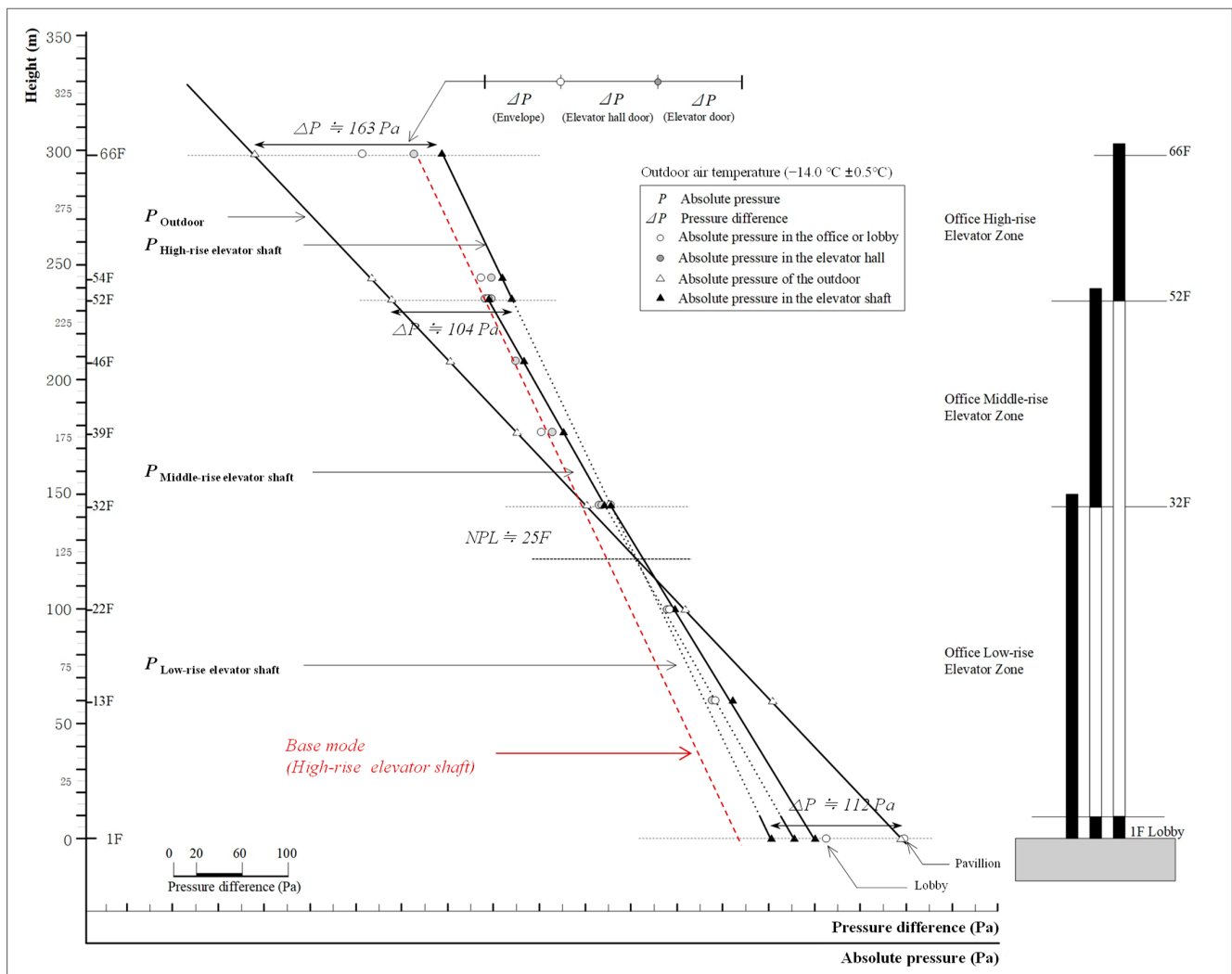


Figure 10. Pressure profile under whole-floor pressurization (Mode 4).

5. Conclusions

This study evaluated the effects of mechanical pressurization on the pressure distribution profile of an actual high-rise building through field measurements to mitigate the problems caused by excessive pressure differences. The pressure distribution in the high-rise building was monitored via a self-developed absolute pressure measurement device installed at the main location of the test building. The test building was a 67-story office building, and absolute pressure measurement devices were installed at 28 points on 10 floors to derive the pressure distribution profile of the test building. The collected data from each floor were used to determine the pressure difference in the main compartments and the horizontal pressure distribution.

The impact of mechanical system pressurization was evaluated by selecting four pressurization modes for operation in the test building. The detailed effects of each mode were evaluated. The mode in which only the lobby zone was pressurized did not significantly affect the pressure variation of the entire building. Most of the modes did not generate a significant impact on the pressure variation. However, the whole-floor pressurization mode was able to reduce the pressure difference across the lobby floor envelope and the elevator door by approximately 18%. This mode also reduced the NPL of the high-rise elevator shaft by approximately 5% and decreased the pressure difference on the lobby floor. The pressure difference on the top floor increased by approximately 20 Pa. Moreover, there were no problems caused by the excessive pressure difference across the elevator doors

on the reference floor due to high TDC values in the office floor envelope and elevator hall compartments.

The impact of the pressurization of the mechanical system on the entire building was evaluated through field measurements, and the results showed that the impact was not significant. The test building had a small envelope area at the lobby level and a few entrance doors. In addition, the TDC value of the lobby floor envelope was high, making it a suitable condition for evaluating the impact of mechanical pressurization. Therefore, the effects of mechanical pressurization may differ in buildings with large podiums or complicated floor plans on the ground floor. The field test was only conducted within a single high-rise building, and, therefore, the effects of mechanical systems in various buildings, such as low-rise podium planning, elevator shaft zoning, and the airtightness of the envelope, should be considered in future studies. These results can be used as a basis for pressure difference sensing to reduce pressure differences in high-rise buildings.

Author Contributions: Conceptualization, K.-H.J. and J.-H.J.; methodology, K.-H.J.; validation, K.-H.J. and J.-H.J.; formal analysis, S.-J.C.; investigation, S.-J.C.; data curation, K.-H.J.; writing—original draft preparation, K.-H.J.; writing—review and editing, K.-H.J., S.-J.C. and J.-H.J.; visualization, K.-H.J. and S.-J.C.; supervision, J.-H.J.; project administration, J.-H.J. All authors have read and agreed to the published version of the manuscript.

Funding: This research received no external funding.

Data Availability Statement: Data are contained within the article.

Acknowledgments: This work was supported by INHA UNIVERSITY Research Grant.

Conflicts of Interest: The authors declare no conflict of interest.

References

1. American Society of Heating, Refrigerating and Air-Conditioning Engineers. Chapter 16: Ventilation and Infiltration. In *ASHRAE Handbook—Fundamentals*; American Society of Heating, Refrigerating and Air-Conditioning Engineers: Atlanta, GA, USA, 2017.
2. Catalina, T.; Iordache, V. IEQ assessment on schools in the design stage. *Build. Environ.* **2012**, *49*, 129–140. [[CrossRef](#)]
3. Varshney, K.; Rosa, J.E.; Shapiro, I.; Scott, D. Air-infiltration measurements in buildings using sound transmission loss through small apertures. *Int. J. Green Energy* **2013**, *10*, 482–493. [[CrossRef](#)]
4. Li, Y.; Duan, S.; Yu, I.T.; Wong, T.W. Multi-zone modeling of probable SARS virus transmission by airflow between flats in Block E, Amoy Gardens. *Indoor Air* **2005**, *15*, 96–111. [[CrossRef](#)] [[PubMed](#)]
5. Hong, G.; Kim, B.S. Field measurements of infiltration rate in high rise residential buildings using the constant concentration method. *Build. Environ.* **2016**, *97*, 48–54. [[CrossRef](#)]
6. Yoon, S.; Song, D.; Kim, J.; Lim, H. Stack-driven infiltration and heating load differences by floor in high-rise residential buildings. *Build. Environ.* **2019**, *157*, 366–379. [[CrossRef](#)]
7. Mao, J.; Yang, W.; Gao, N. The transport of gaseous pollutants due to stack and wind effect in high-rise residential buildings. *Build. Environ.* **2015**, *94*, 543–557. [[CrossRef](#)]
8. Lim, T.; Cho, J.; Kim, B.S. Predictions and measurements of the stack effect on indoor airborne virus transmission in a high-rise hospital building. *Build. Environ.* **2011**, *46*, 2413–2424. [[CrossRef](#)] [[PubMed](#)]
9. Xue, L.; Yuan, S.; He, Q. A comparative study on the influence of ventilation on weather-and fire-induced stack effect in the elevator shafts of a high-rise building. *Fire Technol.* **2018**, *54*, 163–186. [[CrossRef](#)]
10. Jo, J.H.; Lim, J.H.; Song, S.Y.; Yeo, M.S.; Kim, K.W. Characteristics of pressure distribution and solution to the problems caused by stack effect in high-rise residential buildings. *Build. Environ.* **2007**, *42*, 263–277. [[CrossRef](#)]
11. Loveatt, J.E.; Wilson, A. Stack Effect in Tall Buildings. *ASHRAE Trans.* **1994**, *100*, 420–431.
12. Song, D.S.; Lim, H.W.; Lee, J.H.; Seo, J.M. Application of the mechanical ventilation in elevator shaft space to mitigate stack effect under operation stage in high-rise buildings. *Indoor Built Environ.* **2014**, *23*, 81–91. [[CrossRef](#)]
13. Shin, H.K.; Choe, Y.J.; Cho, H.; Jo, J.H. Analysis of the Impacts of Stack Effect in Vertical Shafts with the Condition of Passive Cooling. In Proceedings of the Korean Institute of Architectural Sustainable Environment and Building Systems, Annual Conference in Spring, Anshan, Republic of Korea, 23 March 2012.
14. Xie, M.; Wang, J.; Zhang, J.; Gao, J.; Pan, C.; Li, C. Field measurement and coupled simulation for the shuttle elevator shaft cooling system in super high-rise buildings. *Build. Environ.* **2021**, *187*, 107387. [[CrossRef](#)]
15. Lee, J.; Song, D.; Park, D. A study on the development and application of the E/V shaft cooling system to reduce stack effect in high-rise buildings. *Build. Environ.* **2010**, *45*, 311–319. [[CrossRef](#)]
16. Yu, J.-Y.; Song, K.-D.; Cho, D.-W. Resolving Stack Effect Problems in a High-Rise Office Building by Mechanical Pressurization. *Sustainability* **2017**, *9*, 1731. [[CrossRef](#)]

17. Yu, J.; Kim, A.; Bae, S.; Cho, D.; Kim, K.H. HVAC Operation Schemes and Commissioning Process Resolving Stack Effect Problem and Adjusting According to Changes in the Environment: A Case Study in High-Rise Building in South Korea. *Energies* **2021**, *14*, 2299. [[CrossRef](#)]
18. Koo, S.H. A Strategy for Reducing Stack Pressure Difference in High-Rise Buildings. Master's Thesis, Seoul National University, Seoul, Republic of Korea, 2005.
19. Lim, H.; Seo, J.; Song, D.; Yoon, S.; Kim, J. Interaction analysis of countermeasures for the stack effect in a high-rise office building. *Build. Environ.* **2020**, *168*, 106530. [[CrossRef](#)]
20. Sherman, M. Single-Zone Stack-Dominated Infiltration Modeling. *Indoor Air* **1992**, *2*, 244–256. [[CrossRef](#)]
21. Tamura, G.T.; Wilson, A.G. Building pressures caused by chimney action and mechanical ventilation. *ASHRAE Trans.* **1967**, *73*, 1–12.
22. O'Brien, S.; Cammalleri, V. Stack Effect and Mechanical Exhaust System Impacts on Building Pressures and Envelope Air Leakage. In Proceedings of the Workshop on Building and Ductwork Airtightness Design, Implementation, Control and Durability: Feedback from Practice and Perspectives, Washington, DC, USA, 18–19 April 2013.
23. Shin, H.K. Calculation Method for Determining Air Infiltration of High-Rise Buildings Based on Airtightness and Stack Effect Pressure. Ph.D. Thesis, Inha University, Incheon, Republic of Korea, 2018.
24. Jo, J.H. Prediction of Pressure Distribution Due to Stack Effect in High-Rise Residential Buildings and Evaluation of Its Impact. Ph.D. Thesis, Seoul National University, Seoul, Republic of Korea, 2005; p. 77.
25. Lee, D.S.; Ji, K.H.; Jing, J.; Jo, J.H. Experimental Study on Elevator Door Reopening Problems Caused by Stack Induced Pressure Differences across the Elevator Door in Buildings. *Build. Environ.* **2022**, *221*, 109271. [[CrossRef](#)]
26. Tamblyn, R.T. Coping with air pressure problems in tall buildings. *ASHRAE Trans.* **1991**, *97*, 824–827.

Disclaimer/Publisher's Note: The statements, opinions and data contained in all publications are solely those of the individual author(s) and contributor(s) and not of MDPI and/or the editor(s). MDPI and/or the editor(s) disclaim responsibility for any injury to people or property resulting from any ideas, methods, instructions or products referred to in the content.